

# ANNUAL SUMMARY REPORT

P40: Benefits of Traffic Speed Deflectometer Data in Pavement Analysis (Year 4) 2018-2019

ARRB Project No.: PRP18021

Author/s: Dr Jeffrey Lee & Dr Dominik Duschlbauer

Prepared for: Queensland Department of Transport and Main Roads

30/09/2021

01



# **Summary**

A ground instrumentation site was set up on Deception Bay Road near Brisbane under a NACOE project in 2019. The research supplements a similar ground instrumentation site set up in Western Australia under the WARRIP research initiative. The objective of the project is to provide a high-quality instrumentation site to monitor the pass-by of ARRB's Intelligent Pavement Assessment Vehicle (iPAVe) and also to allow detailed comparison with FWD data. Details of the sensors, their selection, installation and validation, were provided in a previous report.

The key objectives of the current study included:

- developing an improved and reliable method to measure the motion of the embedded sensors
- comparing the deflection from the iPAVe with that of the FWD and validate the correlation developed in previous studies in Queensland and Western Australia
- comparing the output from the embedded array with the iPAVe and FWD
- exploring the feasibility of utilising the embedded array to track the deflection of a range of heavy vehicles
- examining the applications of iPAVe data in other Australian jurisdictions.

Although the report is believed to be correct at the time of publication, the Australian Road Research Board, to the extent lawful, excludes all liability for loss (whether arising under contract, tort, statute or otherwise) arising from the contents of the report or from its use. Where such liability cannot be excluded, it is reduced to the full extent lawful. Without limiting the foregoing, people should apply their own skill and judgement when using the information contained in the report.

The study demonstrated that the instrumentation array can accurately measure the responses from the FWD and iPAVe. The study also demonstrated the practicality of the concept of using the instrumentation array to monitor a range of live traffic vehicles, ranging from light vehicles to multiple-axle heavy vehicles.

The utilisation of the iPAVe data by the different Australian road agencies is also reported.

#### Queensland Department of Transport and Main Roads Disclaimer

While every care has been taken in preparing this publication, the State of Queensland accepts no responsibility for decisions or actions taken as a result of any data, information, statement or advice, expressed or implied, contained within. To the best of our knowledge, the content was correct at the time of publishing.

# **Acknowledgements**

TMR North Coast Region has provided the assistance to identify the ground instrumentation site on Deception Bay Road. Their help is very much appreciated by the project team.

# **Contents**

1	Intro	duction		1	
	1.1	1			
		1.1.1	Recent Work Completed in Western Australia	2	
	1.2	Scope	of Project	3	
		1.2.1	Models for Converting TSD Data	4	
		1.2.2	Details of AUTC Methods	5	
	1.3	Structu	re of the Report	5	
2	Moni	itoring of	TSD Pass-by of Instrumented Site	6	
	2.1 Introduction			6	
	2.2	Site Se	election	6	
		2.2.1	Site Locality and Information from ARMIS Database	6	
		2.2.2	Ground Instrumentation Site	8	
	2.3	Analytic	cal Methods used to Resolve Displacement	10	
3	Resu	ults of Me	easurements	13	
	3.1	.1 Falling Weight Deflectometer (FWD)			
	3.2	Intellige	ent Pavement Assessment Vehicle (iPAVe)	15	
	3.3	Compa	arison between Data Collected by Sensor Array and FWD	16	
	3.4	Compa	arison between Sensor Array and iPAVe Data	17	
	3.5	Compa	arison of all Three Measurement Methods	18	
	3.6	Correla	ation between TSD and FWD	21	
	3.7	Summary of Results			
4	Live	Traffic M	leasurement	25	
5	Use of TSD Data by Other Road Authorities				
	5.1	iPAVe	User Group	28	
	5.2	Transp	ort and Main Roads Queensland (TMR)	28	
	5.3	Main R	loads Western Australia (MRWA)	28	
	5.4	Transp	ort for New South Wales (TfNSW)	29	
6	Cond	clusions		30	
Rof	oronce	20		21	

# **Tables**

Table 2.1:	Pavement conditions and traffic data from ARMIS for Deception Bay Road	7
Table 5.1:	List of iPAVe user organisations that participated in the online forum held on 20 November 2019	28
Table 5.2:	Example of a proposed risk index based on the TSD measurement parameter	
	presented by MRWA	29

# **Figures**

Figure 1.1:	Photograph of Doppler laser in front of the rear dual-tyre axle	1
Figure 1.2:	Geophone with protective cap installed	2
Figure 1.3:	Comparison of selected TSD and FWD deflection bowls (Left: Kwinana Freeway, Right: Leach Highway)	3
Figure 1.4:	Comparison of TSD deflections measured in Perth and Brisbane	3
Figure 1.5:	Pavement deflection velocity under a rolling load	4
Figure 1.6:	Pavement deflection velocity and deflection bowl with deflection slopes (tangents)	4
Figure 2.1:	Aerial photo showing the location of the ground instrumentation site	6
Figure 2.2:	Pavement layers for the westbound left lane along Deception Bay Road	7
Figure 2.3:	Photograph showing the condition of the pavement before installation of ground sensors	8
Figure 2.4:	Layout of ground instrumentation sensors	9
Figure 2.5:	Sensor array geometry and sensor type	9
Figure 2.6:	Typical calibration curve in the frequency domain (magnitude and phase) of an HG6-UB geophone	10
Figure 2.7:	Path of the iPAVe relative to the embedded sensor array (hole location visually marked with masking tape)	10
Figure 2.8:	Weighted velocity time trace (top) and corresponding spectrum (bottom)	11
Figure 2.9:	Calculated unweighted velocities	12
Figure 2.10:	Calculated displacements	12
Figure 3.1:	FWD normalised maximum deflection (D <sub>0</sub> ) near the instrumentation array	13
Figure 3.2:	FWD normalised deflection basin at the instrumentation site	14
Figure 3.3:	Typical velocity and displacement time history of an FWD impact load measured at Deception Bay Road	14
Figure 3.4:	Measured velocities (left) and displacements (right) contour of a TSD pass-by	15
Figure 3.5:	TSD deflections collected from multiple runs along the Deception Bay Road instrumentation site	16
Figure 3.6:	Comparison of maximum deflection reported by an FWD and measured by the instrumentation array	17
Figure 3.7:	Comparison of TSD and deflections measured by the ground instrumentation	17
Figure 3.8:	Comparison of TSD & FWD deflections and deflections measured by the ground instrumentation	18
Figure 3.9:	Illustration of radial and offset distance for a Falling Weight Deflectometer	19
Figure 3.10:	Illustration of transformation radial distance of a TSD measurement	20
Figure 3.11:	Comparison of TSD and deflections measured by the ground instrumentation	20
Figure 3.12:	Comparison of TSD deflection and deflections measured by the ground instrumentation	21
Figure 3.13:	Comparison of TSD and FWD measurements after adjusted for radial distance: Run #3	21
Figure 3.14:	Comparison of TSD and FWD measurements after adjusted for radial distance: Run #4	22
Figure 3.15:	Comparison of TSD and FWD measurements after adjusted for radial distance: Run	
	#7	22

Figure 3.16:	Comparison of TSD and FWD measurements after adjusted for radial distance: Run	
	#8	22
Figure 3.17:	Comparison of TSD and FWD measurements after adjusted for radial distance: Run	
	#9	23
Figure 3.18:	Correlation between the TSD and FWD maximum deflections at Deception Bay Road	23
Figure 3.19:	Correlation between the TSD and FWD curvature (D0-D200) at Deception Bay Road	24
Figure 4.1:	Typical passenger vehicle on Deception Bay Road	25
Figure 4.2:	Example of an unladen three-axle group semi-trailer on Deception Bay Road	26
Figure 4.3:	Example of a bus on Deception Bay Road	26
Figure 4.4:	Example of a loaded flat-bed vehicle on Deception Bay Road	27

# 1 Introduction

# 1.1 Background

In 2014, the Australian Road Research Board (ARRB) acquired a Traffic Speed Deflectometer (TSD) manufactured by Greenwood Engineering. It was then upgraded by ARRB, making it the first integrated road surface and sub-surface condition assessment system in the world. This device is known as the Intelligent Pavement Assessment Vehicle (iPAVe) system. Since then, the TSD has been conducting annual road network surveys in Queensland, Western Australia, New South Wales, and New Zealand.

Several devices are available for pavement structural evaluation at the network level, including the Applied Research Associates (ARA) Rolling Wheel Deflectometer (RWD), Dynatest's RAPTOR™ Rolling Weight Deflectometer (RWD), and the Greenwood Engineering Traffic Speed Deflectometer (TSD).

In Australia, the TSD utilises Doppler lasers to measure the vertical surface velocity of the deflected pavement at six locations along the mid-line of the rear left dual tyres, directly under the rear axle and in front of the tyres at offsets of 100, 200, 300, 600 and 900 mm.  $D_0$  is defined as the deflection directly underneath the rear axle. The seventh Doppler laser, known as the reference laser, is positioned 3,500 mm in front of the rear axle load. The reference laser is presumed to remain relatively unaffected by the load applied by the axles and the vertical pavement deflection velocity of the reference laser is comparatively lower. Figure 1.1 shows a photograph of the different Doppler lasers located ahead of the rear dual-tyre axle.

Various deflection algorithms are available to compute pavement vertical surface deflection, including the Euler-Bernoulli beam model (Rasmussen et al. 2008), the ARRB 'Area Under the Curve' (AUTC) method (Austroads 2014; Muller & Roberts 2013), and the Weibull functional form method (Zofka et al. 2014).

Recent research conducted in the United States (Nasimifar et al. 2016) presented two methods, namely velocity-based and the deflection-based approaches, to estimate the pavement layer moduli for network-level analysis using the TSD. The deflection-based approach, which is to back-calculate the layer moduli from TSD-measured deflections, is being used to explore the use of TSD technology in pavement rehabilitation design in Queensland.



Figure 1.1: Photograph of Doppler laser in front of the rear dual-tyre axle

Source: Lee, Duschlbauer and Chai (2019).

#### 1.1.1 Recent Work Completed in Western Australia

In 2018, a Western Australia Road Research and Innovation Program (WARRIP) project involved the design and installation of two ground-truth instrumentation sites near Perth. The purpose was to improve the understanding of the ground motion imparted on the pavement surface from a TSD pass-by (Lee & Duschlbauer 2019). The instrumentation sites (array of geophones, accelerometers and temperature sensors embedded near the pavement surface) were used to monitor the 'true' surface response when the deflection testing devices travelled over the sensor array. The primary objectives of the project were to:

- allow comparison of deflections measured by the FWD and the TSD
- develop an independent tool to assess the reported deflections from the FWD and TSD
- acquire a better understanding of TSD deflection data, to improve confidence in the adoption of the technology.

A photograph of a geophone sensor used in the project is shown in Figure 1.2.

Figure 1.2: Geophone with protective cap installed



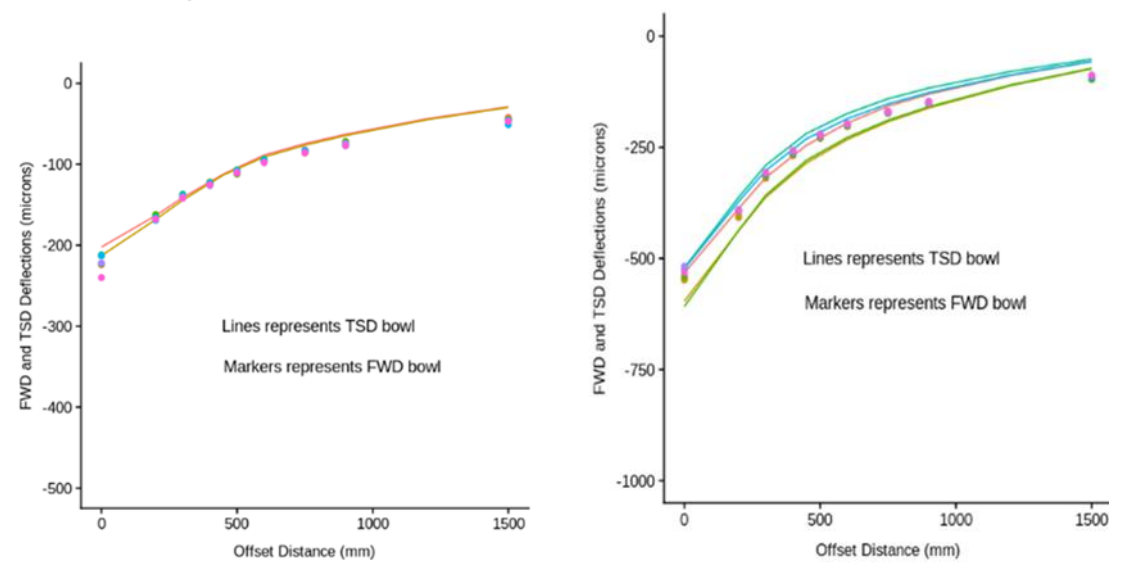
Source: Lee, Duschlbauer and Chai (2019).

Figure 1.3 shows the deflection bowls measured with the embedded array while the TSD was passing over the array (lines) and also the FWD impacts (markers). The results obtained with the embedded array showed good agreement between the results measured by the TSD and FWD. For the Kwinana Freeway site (comprising a full depth asphalt pavement), there was a good match in the front end of the deflection bowl (0 to 600 mm). For the Leach Highway site (comprising asphalt over a cement-bound subbase), the deflection in the front end of the deflection bowls also matched well between 0 mm to 900 mm offset. It was observed that the deflection profiles and correlation varied with pavement type.

To supplement the work carried out in the WARRIP project, Queensland Department of Transport and Main Roads (TMR) sponsored a project under the National Asset Centre of Excellence (NACOE) program which involved the establishment of a ground instrumentation site on Deception Bay Road near Brisbane. The installation on the Deception Bay Road covered the range of deflections which had not been measured during the WARRIP study. Figure 1.4: Comparison of TSD deflections measured in Perth and Brisbane

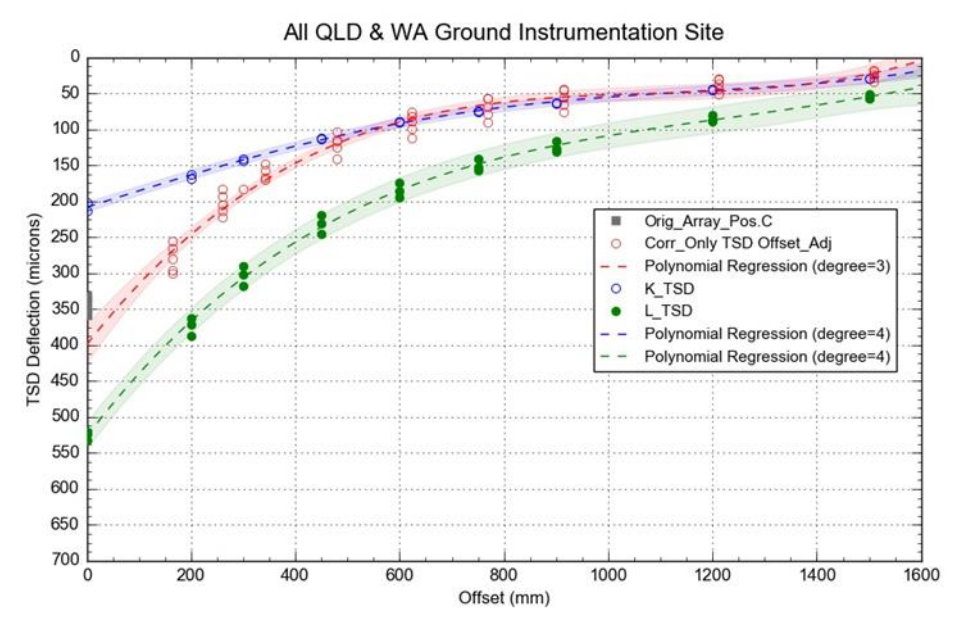
shows the typical TSD deflection bowls measured in Brisbane and Perth.

Figure 1.3: Comparison of selected TSD and FWD deflection bowls (Left: Kwinana Freeway, Right: Leach Highway)



Source: Lee and Duschlbauer (2019).

Figure 1.4: Comparison of TSD deflections measured in Perth and Brisbane



Note: K = Kwinana Freeway; L = Leach Highway.

# 1.2 Scope of Project

The main tasks conducted in Year 4 (2018–19) of the project were as follows:

- Monitor TSD pass-bys on the instrumented site established in Year 3.
- Consult with TMR districts to seek feedback on the draft technical note.
- Liaise with other road agencies to reach agreement regarding the most appropriate approach to the analysis of the TSD data.
- Disseminate knowledge and lessons learnt (deferred to Year 5 study, FY 2019–20).

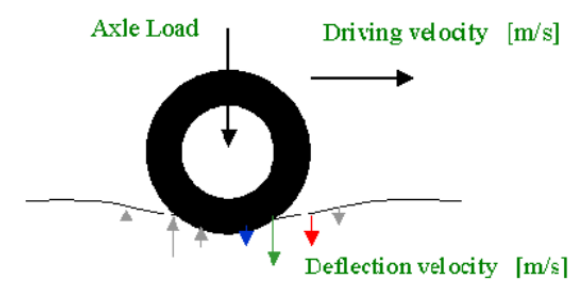
#### 1.2.1 Models for Converting TSD Data

The TSD measures the vertical velocity of the pavement surface while traveling at traffic speed (nominally 80 km/h). A deflection bowl can be obtained by integrating the velocity slopes from each of the doppler lasers. Parameters such as the maximum deflection, curvature, and other structural condition indices can then be derived from the deflection bowl. Two methods are available for converting TSD deflection velocity slope to deflection:

- Euler-Bernoulli beam model (Rasmussen et al. 2008), more commonly known as the 'Greenwood Model'.
- ARRB 'area under the curve' (AUTC) method (Muller & Roberts 2013).

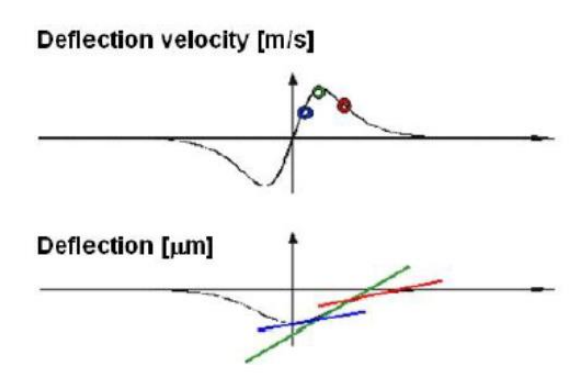
During operations, the Doppler sensors measure vertical velocities of the deflected pavement surface at discrete points and, when divided by the instantaneous vehicle speed, velocity slopes (V<sub>v</sub>/V<sub>h</sub>) at those points (Rasmussen et al. 2008) can be calculated. Figure 1.5 shows the pavement deflection velocity vectors under a rolling wheel. Together with the deflection velocity, the corresponding deflection bowl is shown in Figure 1.6, where deflection slopes (tangents) are displayed. The pavement deflections can be determined by integrating the deflection slope curve using a closed-form solution of a mechanical model such as an elastic beam on a Winkler foundation (Rasmussen et al. 2008).

Figure 1.5: Pavement deflection velocity under a rolling load



Source: Rasmussen et al. (2008).

Figure 1.6: Pavement deflection velocity and deflection bowl with deflection slopes (tangents)



Source: Rasmussen et al. (2008).

The current algorithm being used by the manufacturer is based on a statistical method that fits a curve through the TSD data (Pedersen 2013); it also accounts for asymmetry in the deflection bowl (Nasimifar et al. 2016).

#### 1.2.2 Details of AUTC Methods

The AUTC method was first developed following the initial TSD trials conducted in Australia in 2010 (Muller & Roberts 2013). The method involves fitting the TSD slope measurements and numerically integrating them over the length of the deflection bowl, working towards the wheel load. Details are as follows:

- The base TSD data consists of a set of vertical pavement velocities, referenced against horizontal offsets spaced along the axis of the wheelpath and away from the loading of the dual-tyred truck wheels. This data is termed the velocity profile.
- The value of the velocity at each point is a function of the pavement strength, the offset of the Doppler laser (i.e. the velocity sensor) from the centre point of loading, and the horizontal speed of the TSD (which affects the speed of the vertical loading).
- The slope is the ratio of the vertical and horizontal velocities at each measurement point and the actual
  physical slope of the pavement surface within the deflection bowl centred under the moving TSD's rear
  wheel.
- By plotting slope values against the offsets from the load point as a slope profile curve (analogous to the
  previously mentioned velocity profile), it is possible to show that the cumulative area under the slope profile working from the tail adds up to the vertical deflection at that point where the load is applied.
- The vertical difference between any two deflection points, such as for the bowl curvature,  $(D_0-D_{200})$ , is equal to the area under the slope profile curve between these two points.

# 1.3 Structure of the Report

This report presents a concise summary of the work undertaken in the current year (Year 4) of the study. Section 1 provides the background of the project and the related works carried out in Western Australia. Section 2 outlines the experimental setup; it also provides an improved analysis method for the instrumented site located at Deception Bay Road. The results of the measurements are presented in Section 3 and Section 4. Section 5 provides a report of the workshop held with representatives of TSD users and documents the latest update of the TSD data utilisation in different regions of Australia. Section 6 presents the conclusions of the work.

# 2 Monitoring of TSD Pass-by of Instrumented Site

#### 2.1 Introduction

SLR Consulting Australia Pty Ltd (SLR) was engaged by ARRB to assist with the permanent installation of instrumentation arrays on Deception Bay Road. Details of the sensor selection and installation are reported in Lee and Duschlbauer (2019).

#### 2.2 Site Selection

### 2.2.1 Site Locality and Information from ARMIS Database

Figure 2.1 shows the location of the site, which is near Chainage 5.91 km along the westbound (anti-gazet-tal) left lane of the Deception Bay Road (121).

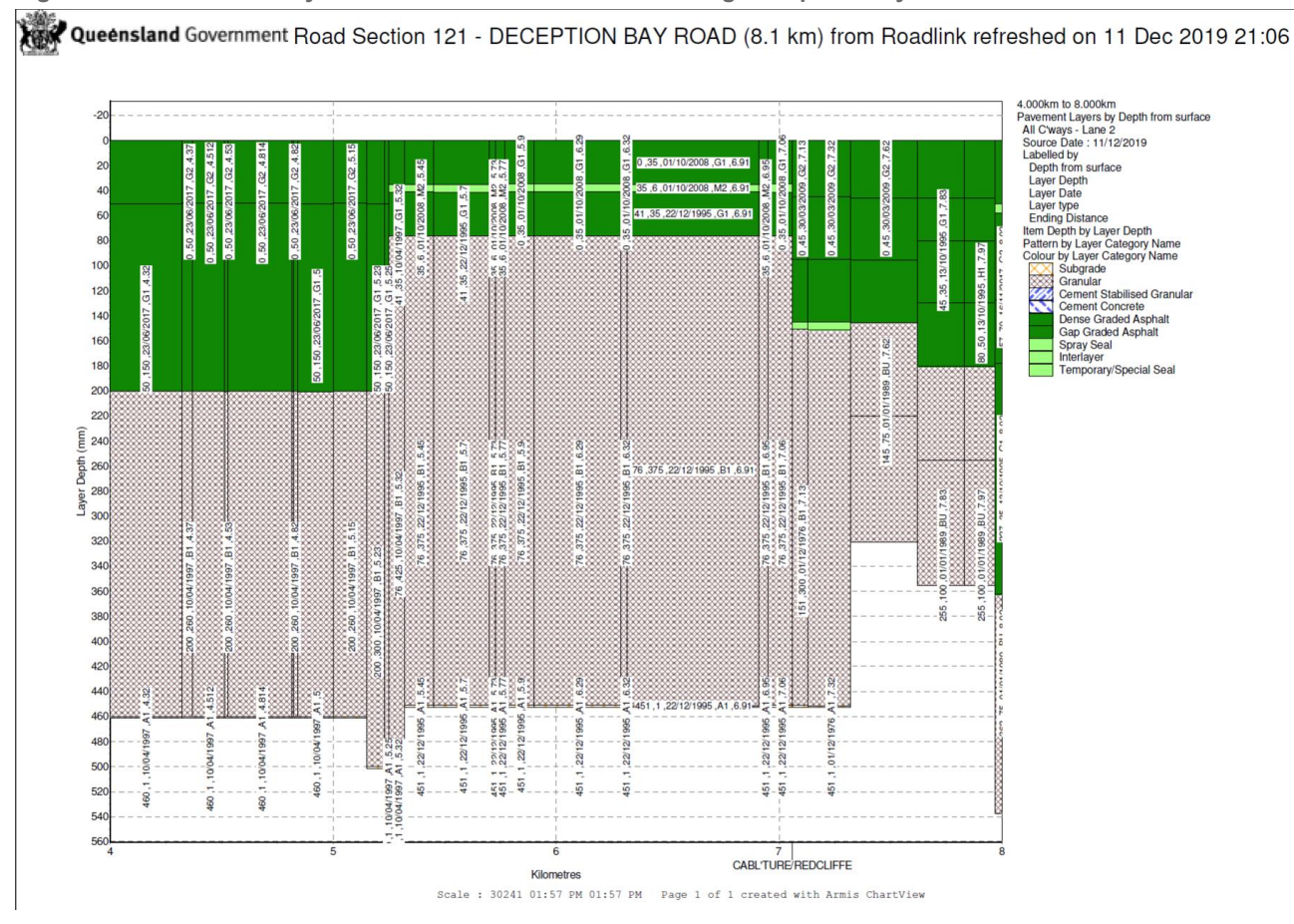
Figure 2.1: Aerial photo showing the location of the ground instrumentation site



Source: nearmap (2019), 'Deception Bay, Queensland', map data, nearmap, Sydney, NSW.

Figure 2.2 is an extract from the TMR ARMIS database; it shows the layers of the pavement where the ground instrumentation site was installed. The pavement construction was consistent and it is in good condition. No maintenance work is currently scheduled for this section of the road.

Figure 2.2: Pavement layers for the westbound left lane along Deception Bay Road



The Deception Bay Road is an arterial road located about 40 km north of the Brisbane CBD. Details of the surface characteristics are summarised in Table 2.1. A photograph showing the site condition before the installation of the ground truth sensors is shown in Figure 2.3.

Table 2.1: Pavement conditions and traffic data from ARMIS for Deception Bay Road

Property			
Surfacing type	Dense-graded asphalt		
Carriageway AADT (2018)	13,864 vehicles/carriageway/day		
Posted speed	70 km/h		
Percentages of heavy vehicles (%)	3%		
TSD deflection D0 (2017)	273.5 microns		
NASSRA roughness (2018)	44		
Rutting (2018)	5.6 mm		
Texture depth (mm)	0.56 mm		
Cracking – All (2018)	8%		
Pavement configuration	35 mm asphalt surfacing 35 mm asphalt binder layer 375 mm granular base Subgrade		

Deception Bay Road is two lanes per carriageway and the posted speed limit is 70 km/h. The number of heavy vehicles is approximately 3% of the total traffic. Based on the information available from the ARMIS database, the pavement comprises 70 mm of asphalt, placed in two layers, over 375 mm of unbound granular pavement. The NAASRA roughness count was reported to be 44 counts/km, the average rut depth was 5.6 mm, and the TSD maximum deflection was 0.27 mm. The array is located along a straight section of road to allow the TSD to align with the instrumented array and maintain a consistent test speed. No asphalt resurfacing work is scheduled in the next five years. This was essential for this work, because the installed sensors were located within the asphalt wearing course and can be damaged during the next asphalt resurfacing work.

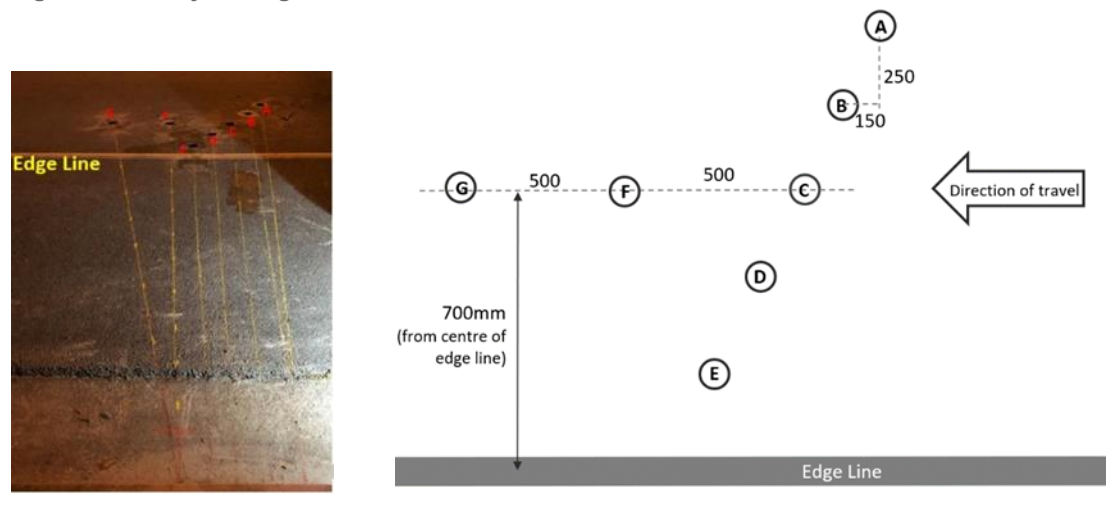




#### 2.2.2 Ground Instrumentation Site

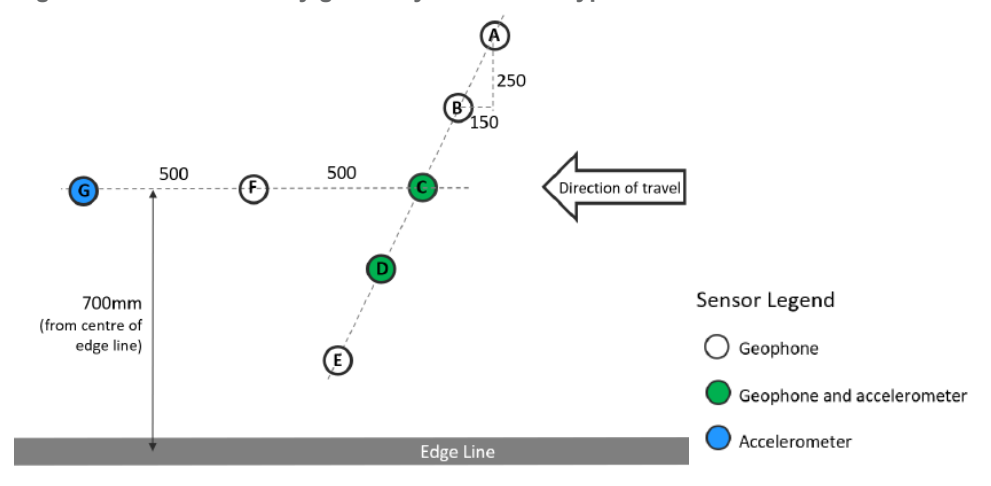
Both geophones (sensors measuring velocities) and accelerometers (sensors measuring accelerations) were installed at night between 1 and 3 October 1, 2019. A a schematic diagram of the instrumentation array is shown in Figure 2.4. Based on previous experience with similar instrumentation sites in Western Australia (Lee et al. 2019), the sensor array was strategically designed to maximise the number of TSD wheels travelling directly over the array. The array extends  $\pm$  250 mm laterally from what was considered the most frequently travelled wheelpath. The array extends 1,000 mm in the longitudinal direction.

Figure 2.4: Layout of ground instrumentation sensors



Single geophones were installed in holes A, B, E, and F, whilst Holes C and D accommodate both geophones and accelerometers, They are designed to validate the measurement accuracy of both sensors. Hole G, which has a single high-precision accelerometer located 1 m away from hole C, was used to provide high-accuracy acceleration history as well as the accurate determination of the instantaneous speed of the iPAVe at the time it travels over the array. Details of the sensor array geometry and sensor type are summarised in Figure 2.5.

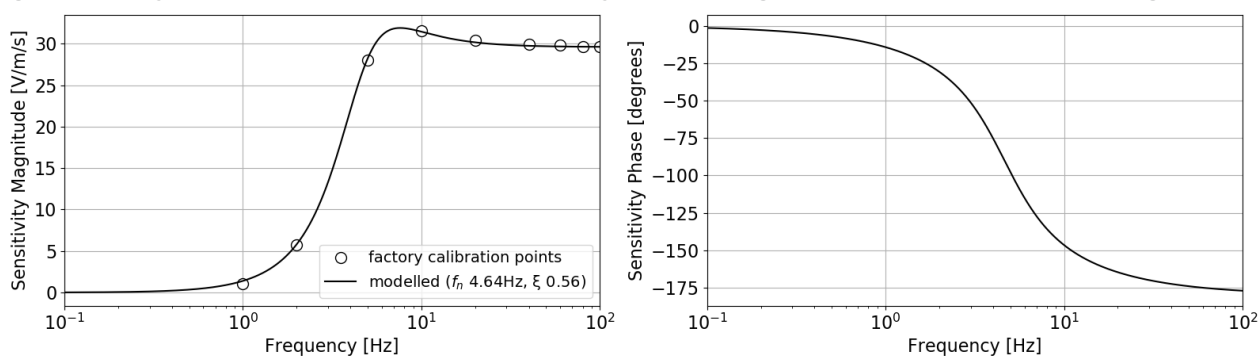
Figure 2.5: Sensor array geometry and sensor type



It was identified early in the project that one of the challenges would be to convert the velocity and acceleration data to displacement data. This was achieved by integration. Each integration step in the analysis introduces a constant (DC shifts) which can result in the deflection drifting off from zero over time. This needed to be taken into account when developing the current analysis method to minimise this effect.

HG6-UB geophones, manufactured by HGS (India) Limited, were selected for the study. The model range selected was a nominal sensitivity of 30 V/m/s, a nominal corner frequency of 4.5 Hz, and a nominal damping ( $\xi$ ) of 0.56. A typical calibration curve is shown in Figure 2.6.

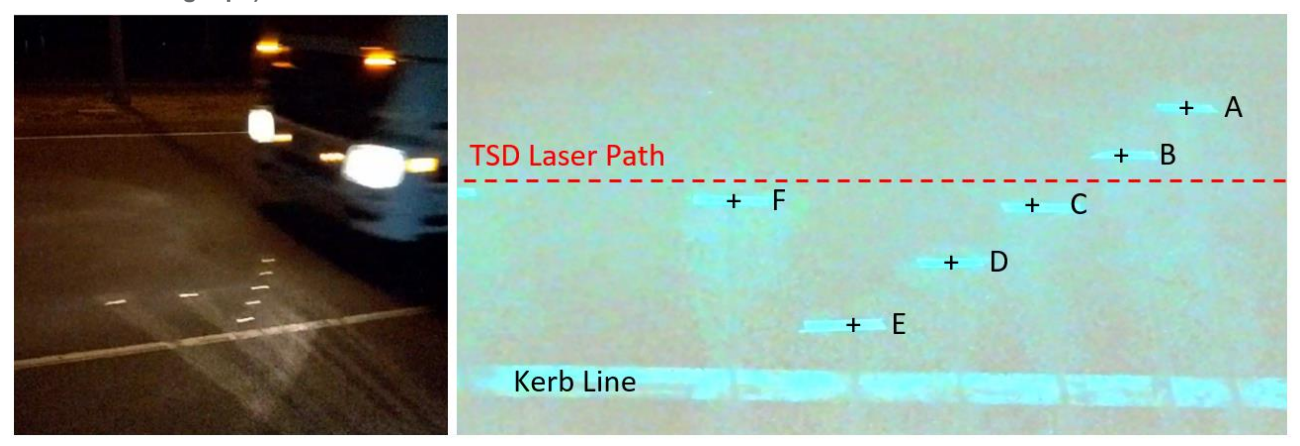
Figure 2.6: Typical calibration curve in the frequency domain (magnitude and phase) of an HG6-UB geophone



# 2.3 Analytical Methods used to Resolve Displacement

For the initial investigative run, the iPAVe truck travelled at a speed of 65 km/h over the array. The position of the laser beam (which was visible on the pavement) was located by studying slow-motion videos. The wheelpath was defined as the centreline of the dual-tyre rear wheels. The pass-by is indicated in red on the right-hand side of Figure 2.7. The centreline of the iPAVe rear dual tyres travelled over the array between geophones B and C, with the offset from geophone C estimated to be 150 mm (i.e. geophone C is the closest geophone).

Figure 2.7: Path of the iPAVe relative to the embedded sensor array (hole location visually marked with masking tape)



The sensors' outputs were recorded synchronously with a 24-bit data acquisition system in DC-coupled mode. The sampling frequency for the run was 5,000 Hz. The top graph in Figure 2.8 shows the 'weighted velocity' as measured by the geophone in hole C. The weighted velocity is directly proportional to the measured voltage from the sensor, the proportionality being the geophone's nominal sensitivity. The three axles travelling over the array are discernible visually and their spacing allowed for calculating the velocity of the iPAVe truck. The iPAVe's speed was also recorded by its onboard GPS; the two speeds matched exactly.

As shown in Figure 2.8, the sensitivity (or calibration factors) of the geophone varied with frequency (i.e. the signal measured directly from the sensor was non-linear). To account for the non-linear nature of the geophone, calibration factors (such as that shown in Figure 2.8) needed to be applied to convert the weighted velocity into the unweighted velocity. The unweighted velocity was used to compute the surface deflection.

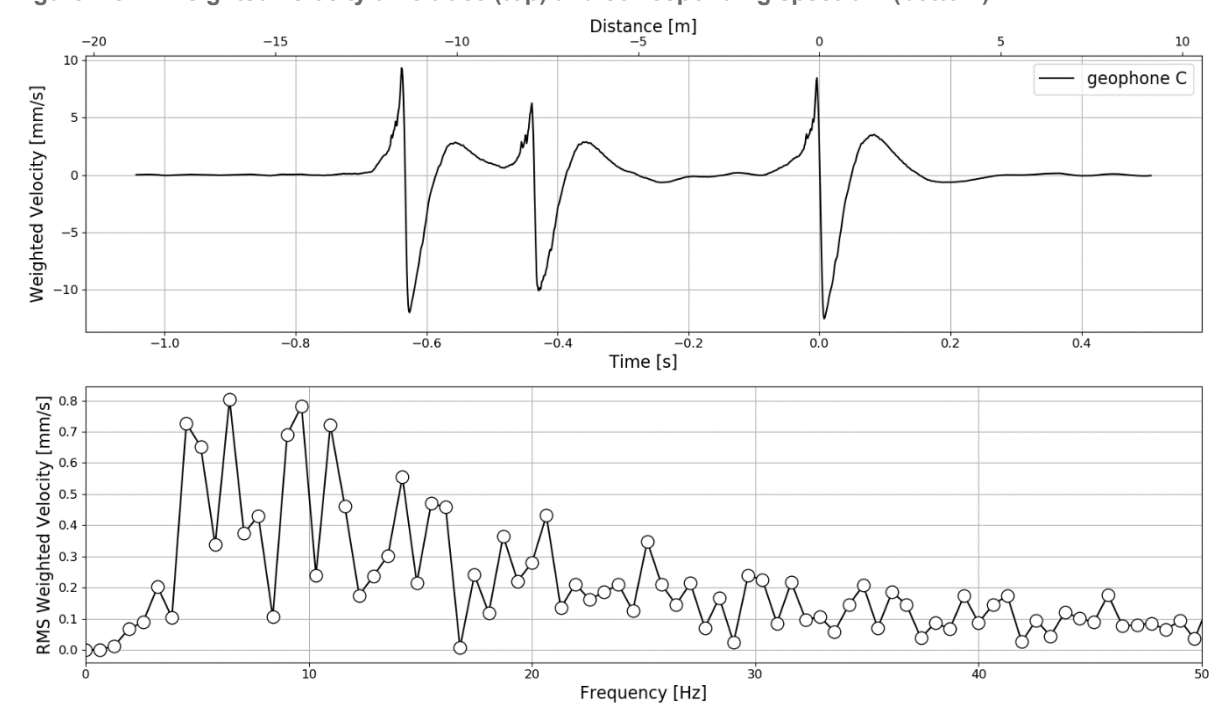


Figure 2.8: Weighted velocity time trace (top) and corresponding spectrum (bottom)

To calculate unweighted velocities and the associated deflections the following analysis were taken:

Select a time segment: The effect of time slices of different durations was a focus of interest in this study.
 Short time slices, coinciding with only one axle rolling over the sensor, and longer time slices, which included all three axles of the iPAVe, were studied.

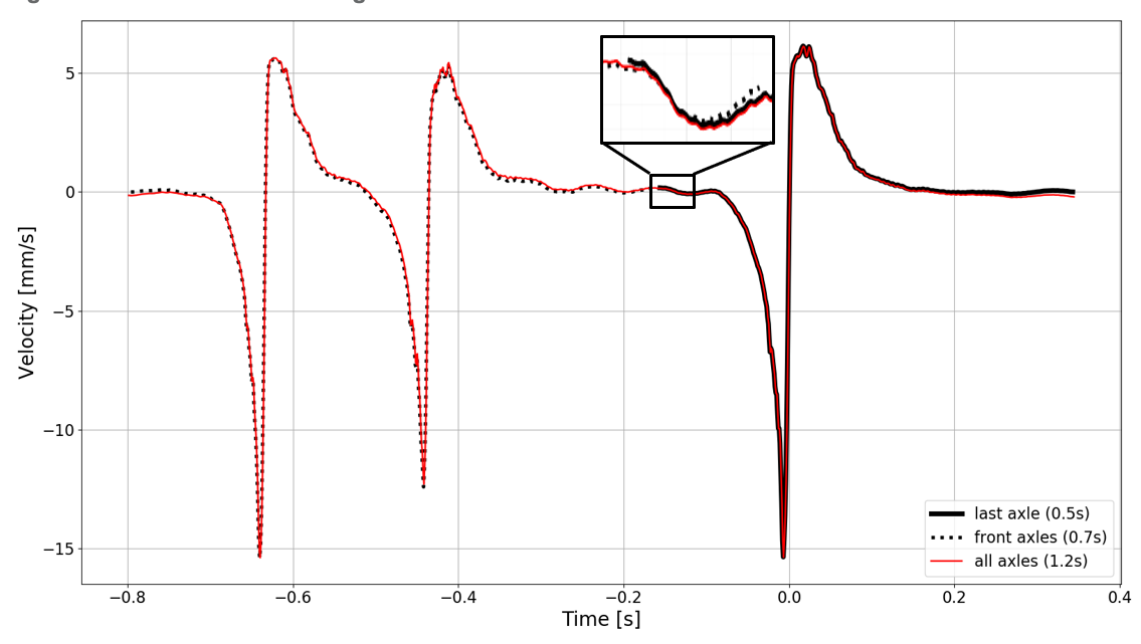
For each time segment, the following post-processing steps were taken:

- The measured voltage pass through a high pass filter to remove any low frequency component.
- The voltage was converted to an unweighted velocity using the inverse Fast Fourier Transform (FFT) method. In this method, the complex FFT of the time signal at each frequency bin is divided by the geophone's complex transmissibility and then converted back into the time domain using the inverse FFT.
- The unweighted velocity was then integrated into displacements in the time domain.

These analysis steps were carried out for each geophone individually using the individual factory calibration sheet. The results for geophone C (its weighted velocity) are presented in Figure 2.8.

Figure 2.9 shows the time traces of the unweighted velocities for all three axle groups. In this case, the front axles accounted for 0.7 seconds of the time record, whilst the last axles (where the TSD deflections were measured) accounted for 0.5 seconds of the time record. The differences in the unweighted velocities when using a different length of time-trace were not significant. However, when the unweighted velocities were converted into displacements (as shown in Figure 2.10), the 'DC-shift' anomaly became more pronounced when the results obtained from the full time-trace (1.2 seconds) were compared with the rear axle time-trace (0.5 seconds). When using a full time-trace, the reported displacements can become positive, i.e. the pavement surface was being 'up-lifted' when the iPAVe drove past. This was simply caused by the error introduced during the FFT conversion step.

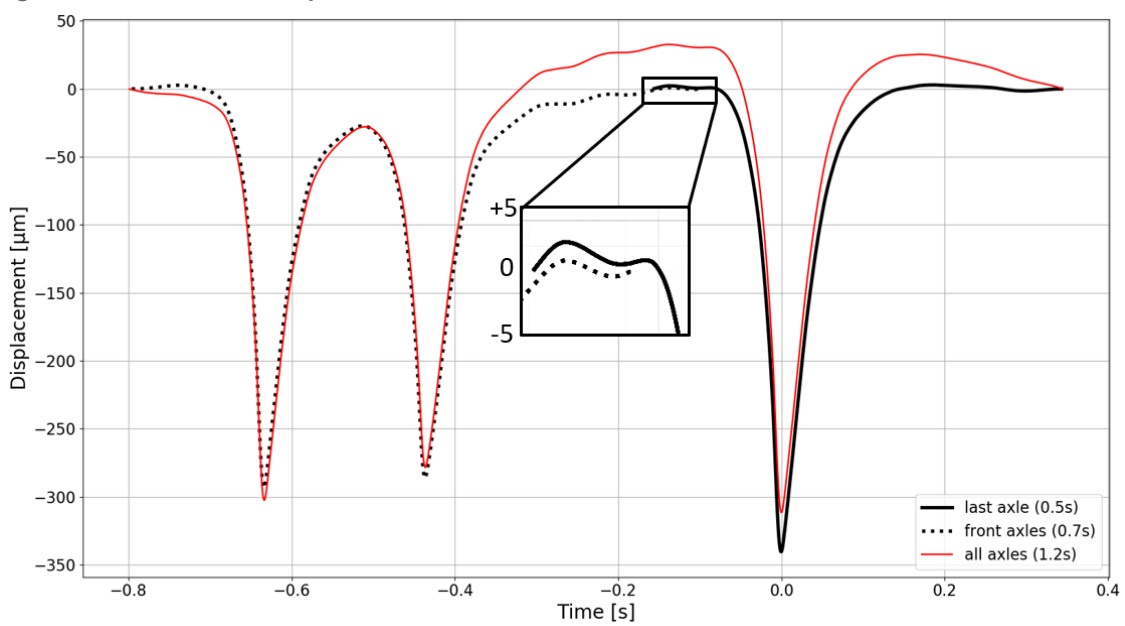
Figure 2.9: Calculated unweighted velocities



However, the integration of the longer time segment (comprising all three axles, red curve) yielded noticeably different results. They were affected by what could be called the effects of a 'low frequency drift'. Hence, it was concluded that the best way to avoid the 'up-lift' artifact in this analysis was to only use a time-trace consisting of only the last rear axle.

This is a well-known problem and arises from a combination of two effects: namely, the geophone unweighting procedure, which amplifies low-frequency energy below the geophone's corner frequency. This is further compounded by the subsequent integration to displacements. The analysis method proposed here effectively minimised the error caused by the integration and the 'up-lift'.

Figure 2.10: Calculated displacements



# 3 Results of Measurements

After the installation of the ground instrumentation sensors, closely-spaced FWD drops and multiple runs of the iPAVe were conducted. The ground-instrumentation array was monitored and time history was recorded during all FWD and iPAVe testing. This section presents the results from all three different measurements.

# 3.1 Falling Weight Deflectometer (FWD)

FWD deflection testing with a target impact load of 50 kN (normalised to 708 kPa) was conducted in the vicinity of the instrumentation array. Figure 3.1 and Figure 3.2 show the normalised FWD maximum deflections and deflection bowls for the same test area. The instrumentation array was located at Chainages 0 m. The magnitude and shape of the bowls aligned with the typical performance of the pavement structure reported in ARMIS.

The maximum deflection profile shown in Figure 3.1 confirmed that the pavement between Chainages –20 m and +20 m are relatively uniform with an average deflection of around 400 microns under the 50 kN test load.

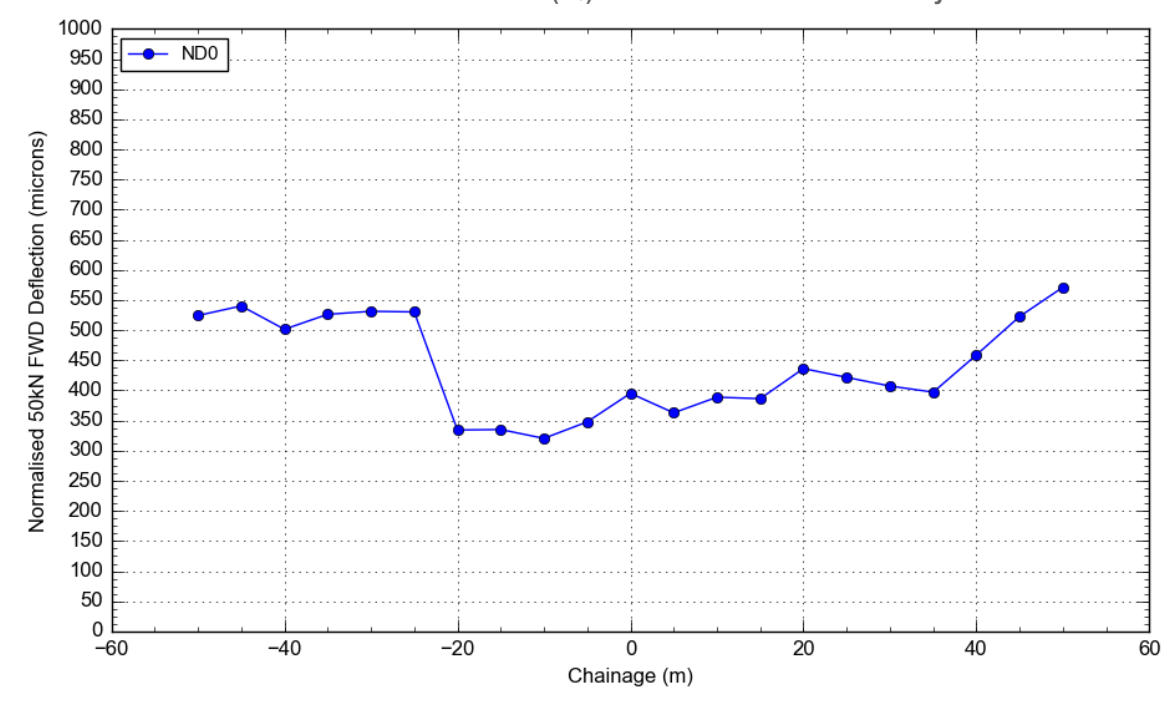


Figure 3.1: FWD normalised maximum deflection (D<sub>0</sub>) near the instrumentation array

Figure 3.2: FWD normalised deflection basin at the instrumentation site

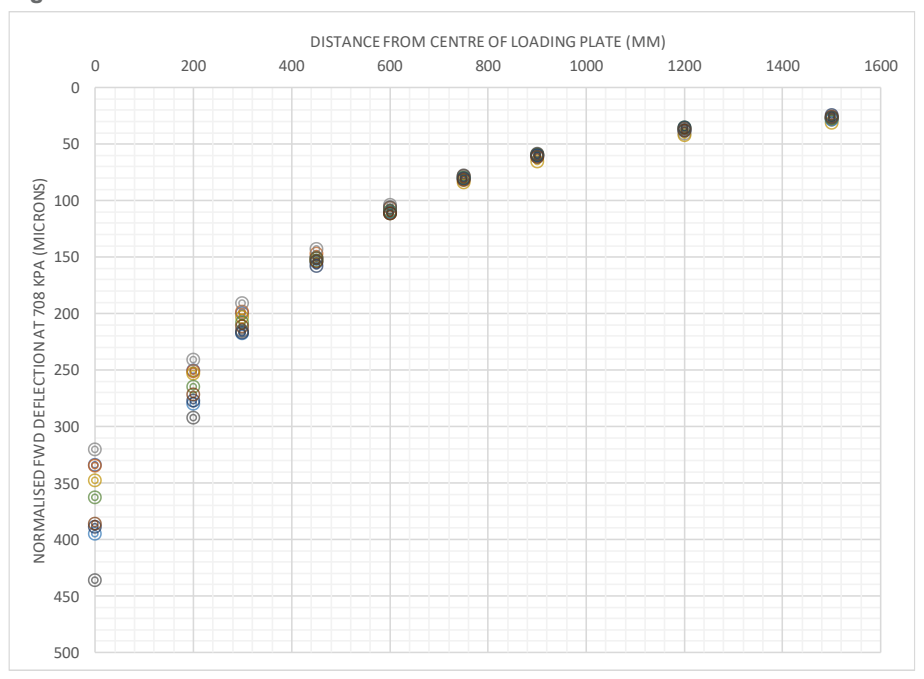
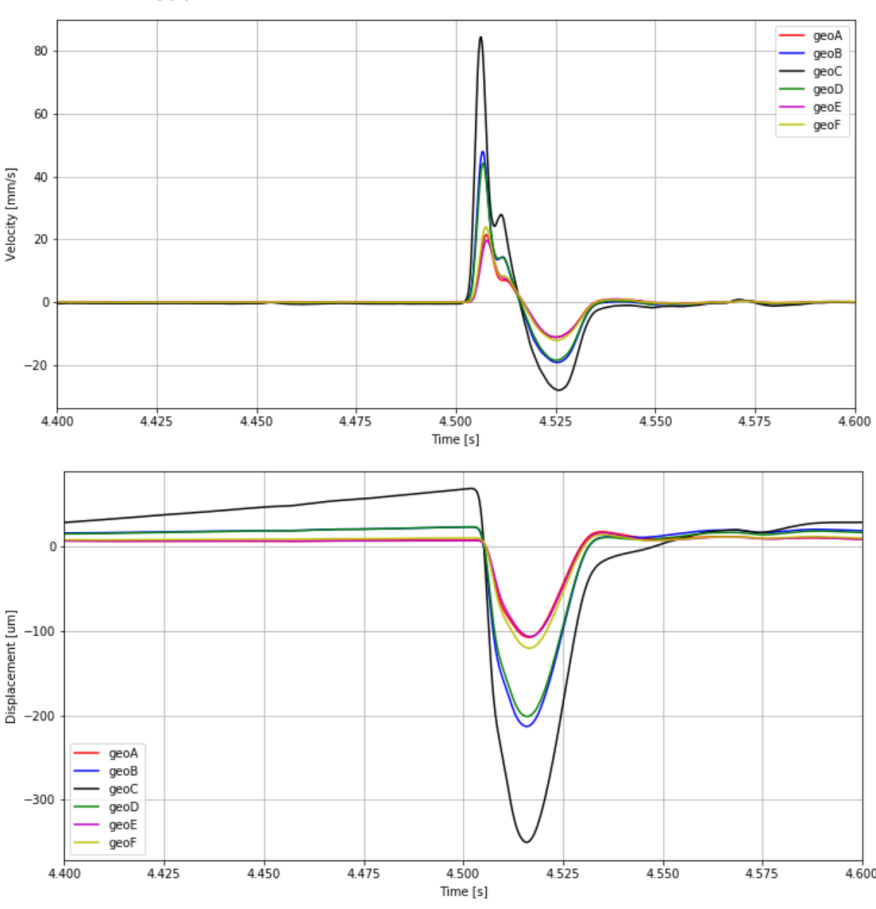


Figure 3.3 shows a time history of all sensors embedded in the instrumentation array when the FWD loading plate was aligned at the centre of the array (i.e. Location C is shown at Chainage 0 m in Figure 3.2). The graph shown at the top of Figure 3.3 is the measured velocity, whilst the bottom graph shows the displacement time history. As anticipated, the peak velocity was recorded at Location C, with the motion reducing as the radial offset distance increased.

Figure 3.3: Typical velocity and displacement time history of an FWD impact load measured at Deception Bay Road



One key difference in the instrumentation array design in Queensland compared to the array used in Perth was the lateral layout of the sensors. All the sensors installed in Perth were located along a linear line on the left wheelpath, whilst, in Queensland, three sensors were installed along the left wheelpath, but four additional sensors were placed at lateral offsets of250 mm and 500 mm on each side of the left wheelpaths (as illustrated in Figure 2.5). The primary advantage of this approach was that it enabled the travel path of the rear axle tyres to be captured, even if the iPAVe was not perfectly aligned with the left wheelpath. The second advantage was that the deflection 2D velocity and displacement contours, as shown in Figure 3.4, could be measured and linearly interpolated using the data points collected from each sensor.

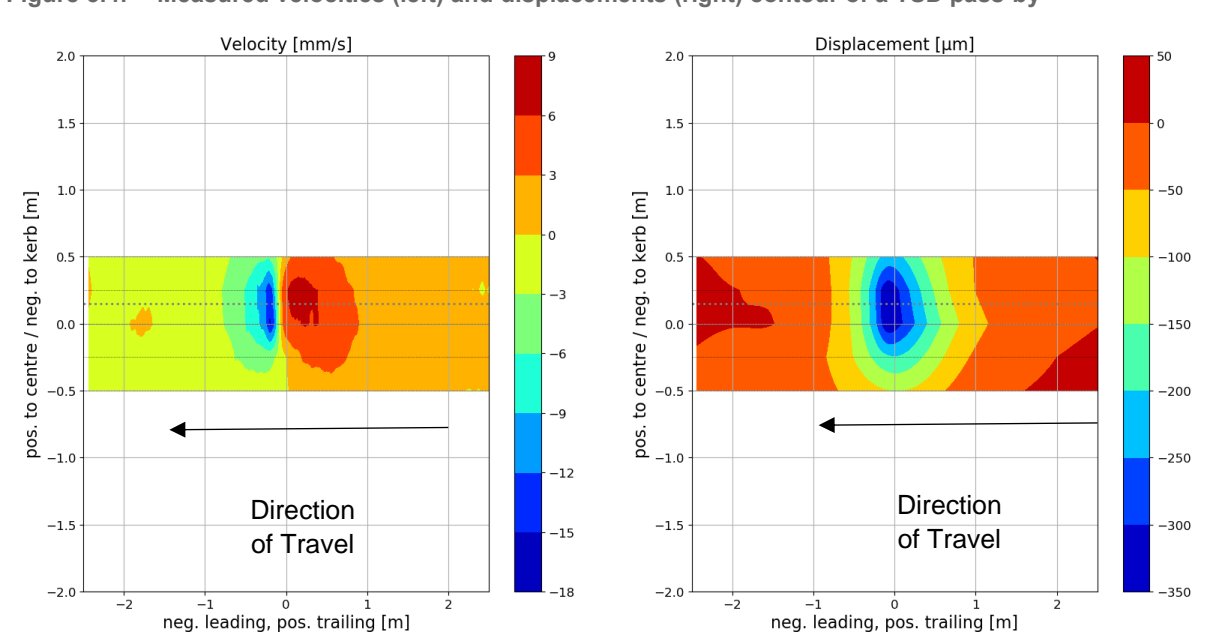


Figure 3.4: Measured velocities (left) and displacements (right) contour of a TSD pass-by

# 3.2 Intelligent Pavement Assessment Vehicle (iPAVe)

Multiple runs using the iPAVe were undertaken on the night of 18 November 2019. In order to study the variability of the iPAVe measurements and the influence of test speed on the deflection, multiple runs of the iPAVe were carried out. Some runs are not reported here because of the alignment issue of the iPAVe with the centreline of the instrumentation array. Plots showing the variation of load, speed, and maximum deflections measured in runs no. 3, 4, 7, 8, and 10 are shown in Figure 3.5.

iPAVe data was collected at two nominal operating speeds: 50 km/h and 70 km/h. The results of the testing were as follows:

- The dynamic loading measured by the on-board load cells at 70 km/h fluctuated more than at 50 km/h, with the load variability generally ranging between 97.5% and 100%.
- The maximum deflection (D<sub>0</sub>) measured by the TSD ranged between 200 and 300 microns within the zone 20 m before and after the instrumentation array. This can partly be explained by the load fluctuation measured during testing.

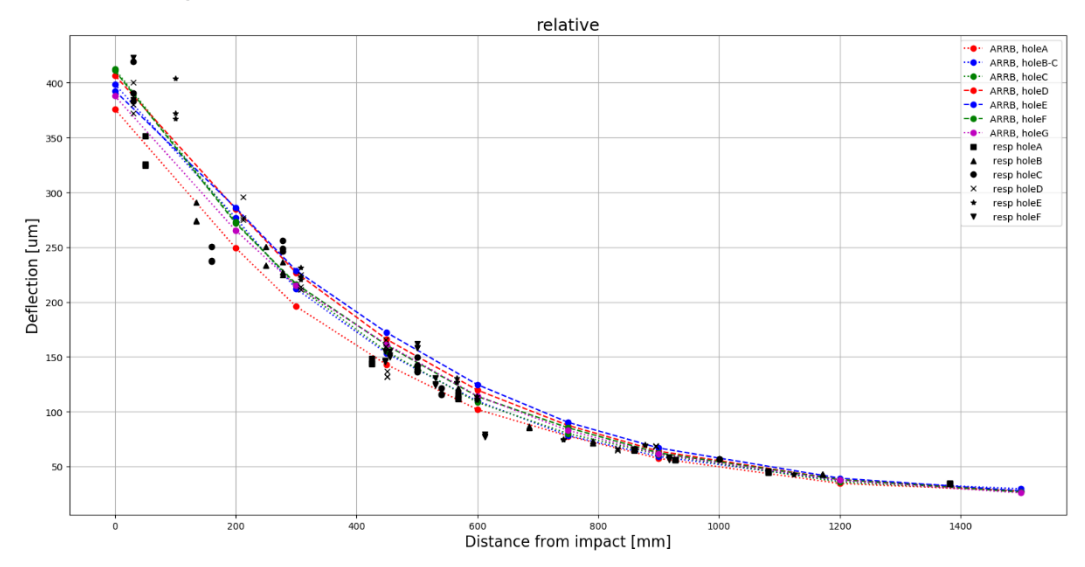
A boxplot with jitter A boxplot with jitter 1.10 -80 -1.05 % of 10T load speedcheck 60 . 1.00 0.95 50 -0.90 40 . 10 10 TSD Run ID TSD Run ID TSD D0 Plot for Deception Bay Road runid 400 Run % of 10T load 300 00 200 8 8 10 10 100 0.8 0 10 20 -20 -10 10 20 -20 -10 0 % of 10T load Chainage

Figure 3.5: TSD deflections collected from multiple runs along the Deception Bay Road instrumentation site

# 3.3 Comparison between Data Collected by Sensor Array and FWD

The FWD deflections were compared to the output of the different embedded sensors. It can be seen from Figure 3.6 that there was very good agreement between the magnitude of the deflections measured by the FWD and the instrumentation array. This cross-check provided confidence to the project team that the instrumentation array was functioning properly.

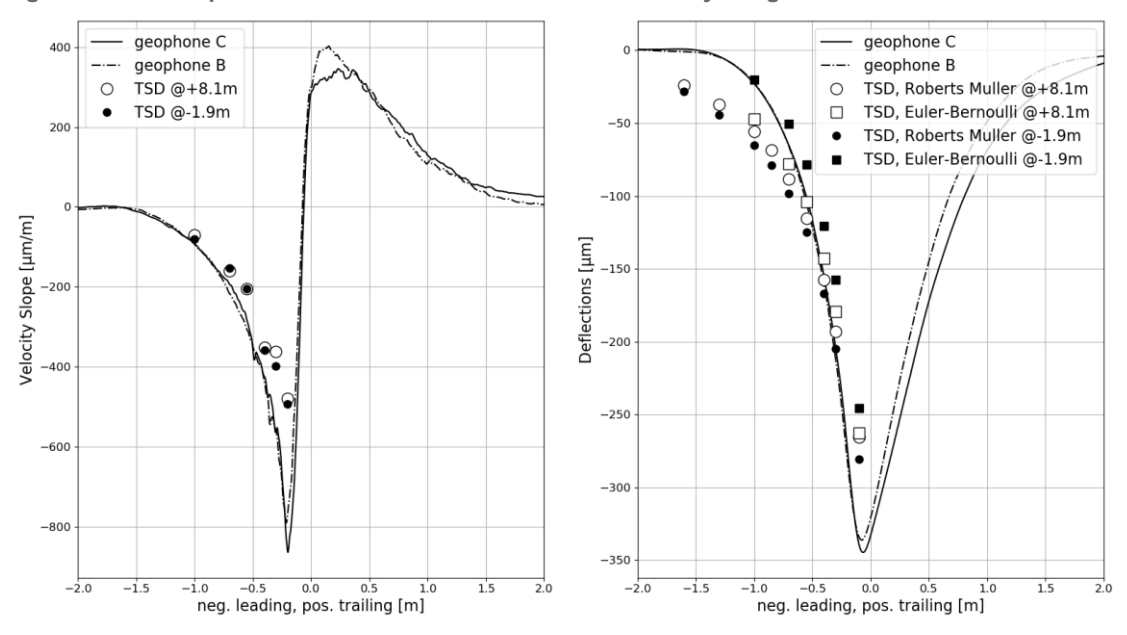
Figure 3.6: Comparison of maximum deflection reported by an FWD and measured by the instrumentation array



# 3.4 Comparison between Sensor Array and iPAVe Data

Similar to the comparison between the instrumentation array and the FWD, the iPAVe velocity and deflection measurements were compared with the motion measured by the instrumentation array, and the results are shown in Figure 3.7. It is worth noting that, during this run, the iPAVe did not run over the sensor directly but was offset by approximately 70 mm. Therefore, a perfect match of the deflections could not be expected. Nevertheless, it can be observed that the measurements were in reasonably good agreement.

Figure 3.7: Comparison of TSD and deflections measured by the ground instrumentation



#### 3.5 Comparison of all Three Measurement Methods

A total of three sets of measurements were made at the Deception Bay Road site: the iPAVe, the FWD, and the sensors embedded in the pavement within the instrument array. Figure 3.8 shows all the measurements collected with the data plotted against the offset distance (i.e. the distance between the centre of the rear axle and the individual sensor, in the direction of travel). Based on the plot, it was observed that the FWD measured deflections under a 50 kN load were approximately 25% higher than the iPAVe deflections. This is consistent with the findings from previous studies in Queensland and Western Australia.

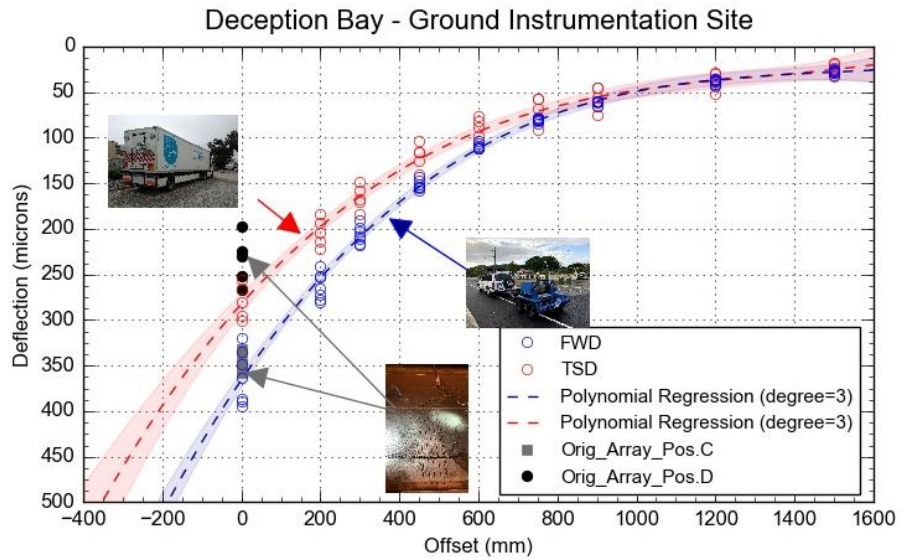


Figure 3.8: Comparison of TSD & FWD deflections and deflections measured by the ground instrumentation

To understand the differences between the three types of measurements, it is suggested that the disagreement can partially be compensated if the results are plotted against the radial offset distance instead of the offset distance in the direction of travel shown in Figure 3.8.

The differences between the radial distance from the loading point to each of the sensors in an iPAVe and an FWD is illustrated in Figure 3.9 and Figure 3.10. A schematic diagram of an FWD measurement is shown in Figure 3.9 . As the FWD only applies the load to a single circular loading plate at the centre of the trailer, the offset distance between the centre of the load to each sensor is the same as the radial distance (denoted as 'R') in the Figure.

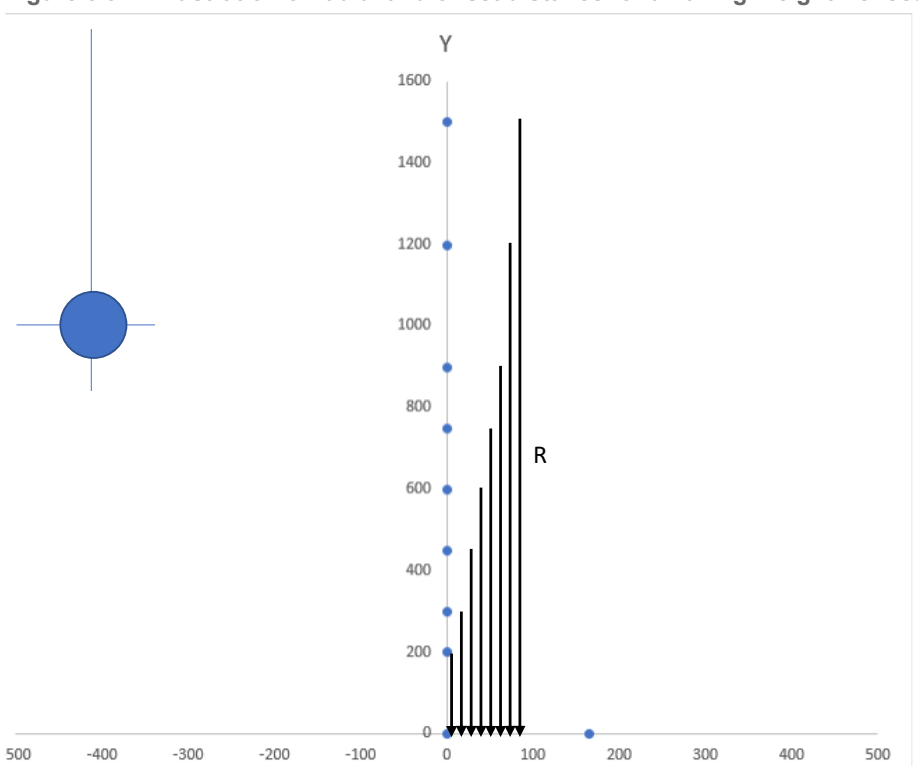


Figure 3.9: Illustration of radial and offset distance for a Falling Weight Deflectometer

Similarly, an illustration of the transformation radial distance of a TSD measurement is shown in Figure 3.10. The iPAVe applies the load at the rear axle fitted with dual tyres on each side. Assuming most of the load measured by the Doppler lasers is from the left half of the axle, it is clear that the offset distance in the direction of travel (denoted as 'Y') is different to the radial offset distance (denoted as 'R'). The difference between 'Y' and 'R' is largest near the vicinity of the dual-tyres and diminishes as the distance increases.

In a linear elastic medium, and using the Boussinesq theory, the surface deflection decreases as the radial distance between the point load increases. Following the same concept, a closer agreement between the FWD and iPAVe data can be obtained by simply plotting the deflection against the radial distance. The relationship after this transformation is shown in Figure 3.11.

It follows that the same radial distance adjustment can be applied to the embedded sensor in the array, and the results are presented in Figure 3.12.

Figure 3.10: Illustration of transformation radial distance of a TSD measurement

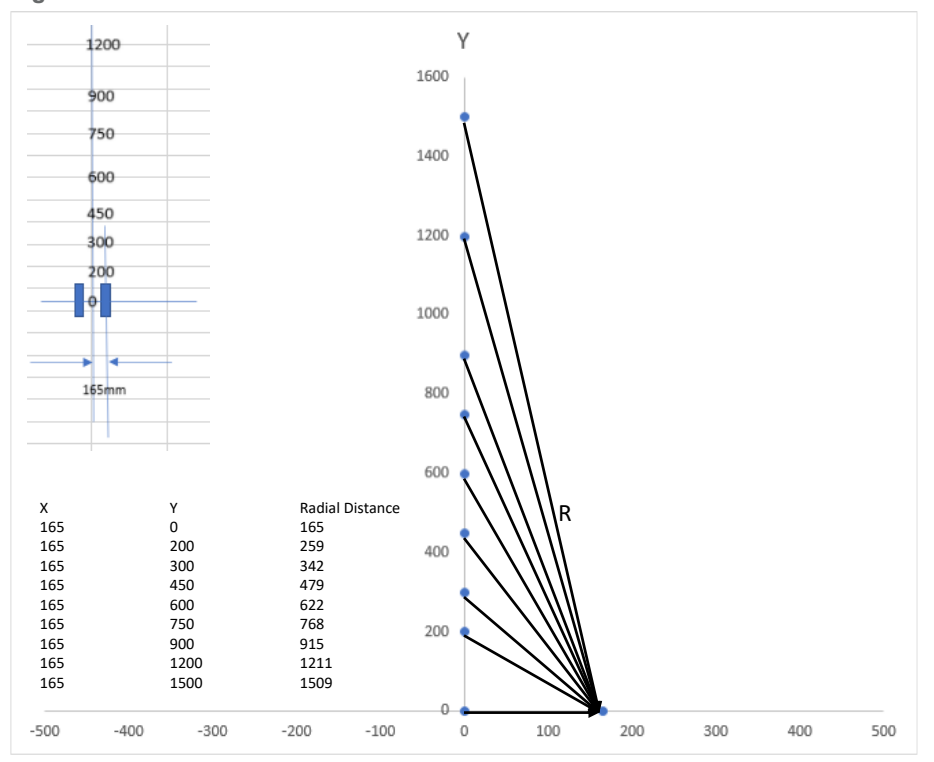


Figure 3.11: Comparison of TSD and deflections measured by the ground instrumentation

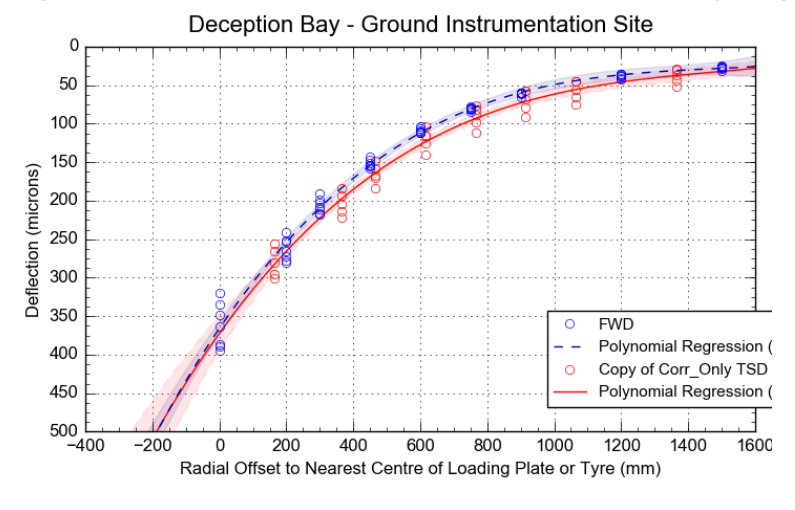
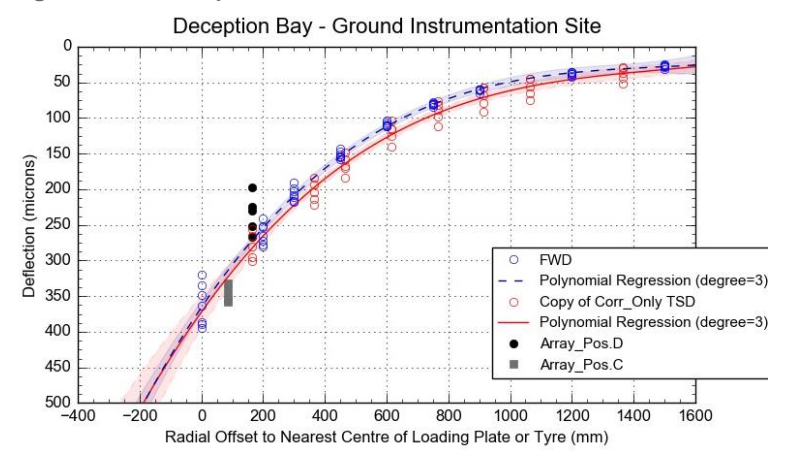


Figure 3.12: Comparison of TSD deflection and deflections measured by the ground instrumentation



#### 3.6 Correlation between TSD and FWD

The same concept was then applied to iPAVe runs no. 3, 4, 7, 8, and 10; as shown in Figure 3.13, Figure 3.14, Figure 3.15, Figure 3.16 and Figure 3.17, respectively. It was found that the adjustment corrected the shape of the deflection bowls and significantly reduced the discrepancy between the two devices. This adjustment was only applied to the Deception Bay Road data collected in Queensland. More data is needed to prove the validity of this transformation.

Figure 3.13: Comparison of TSD and FWD measurements after adjusted for radial distance: Run #3

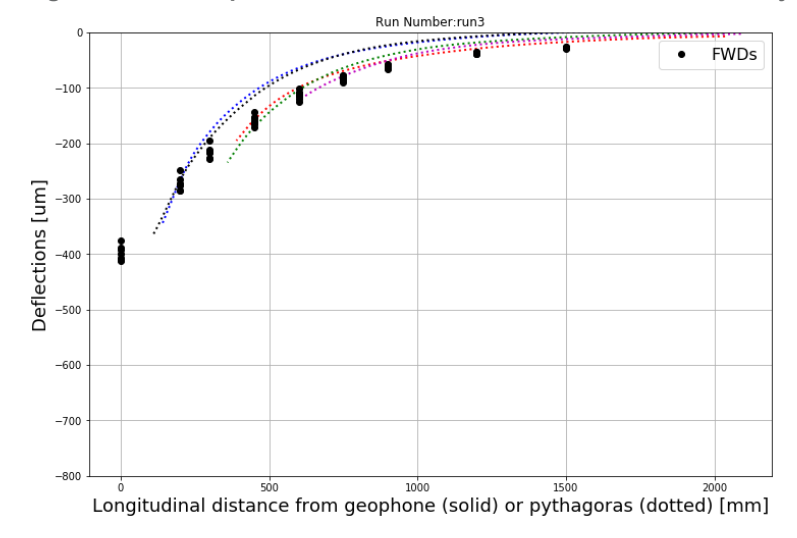


Figure 3.14: Comparison of TSD and FWD measurements after adjusted for radial distance: Run #4

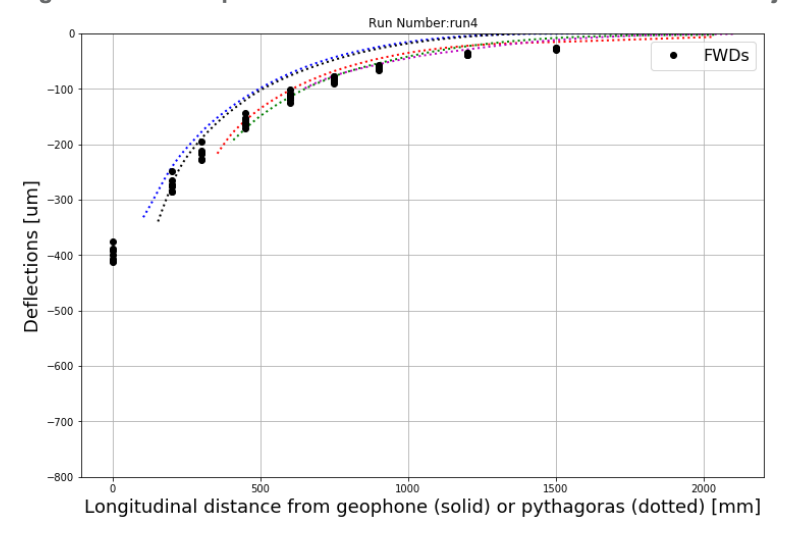


Figure 3.15: Comparison of TSD and FWD measurements after adjusted for radial distance: Run #7

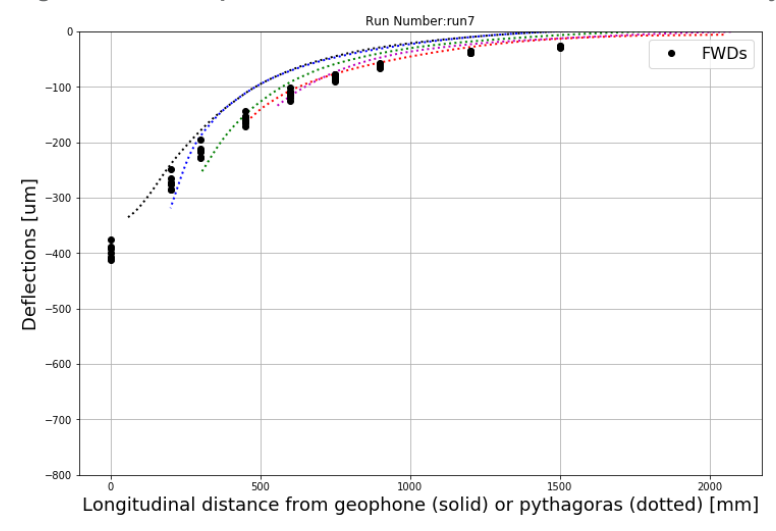


Figure 3.16: Comparison of TSD and FWD measurements after adjusted for radial distance: Run #8

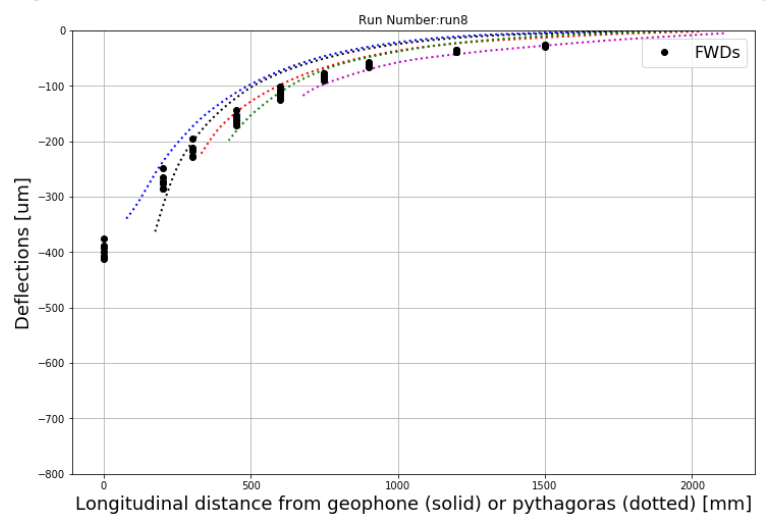
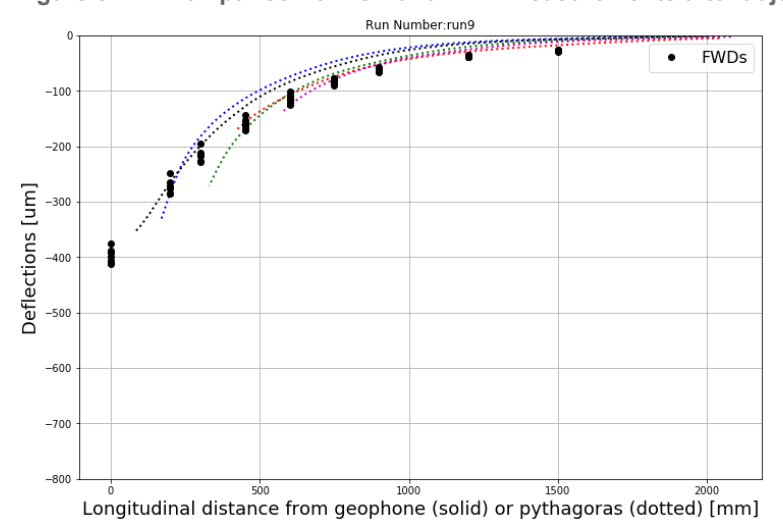
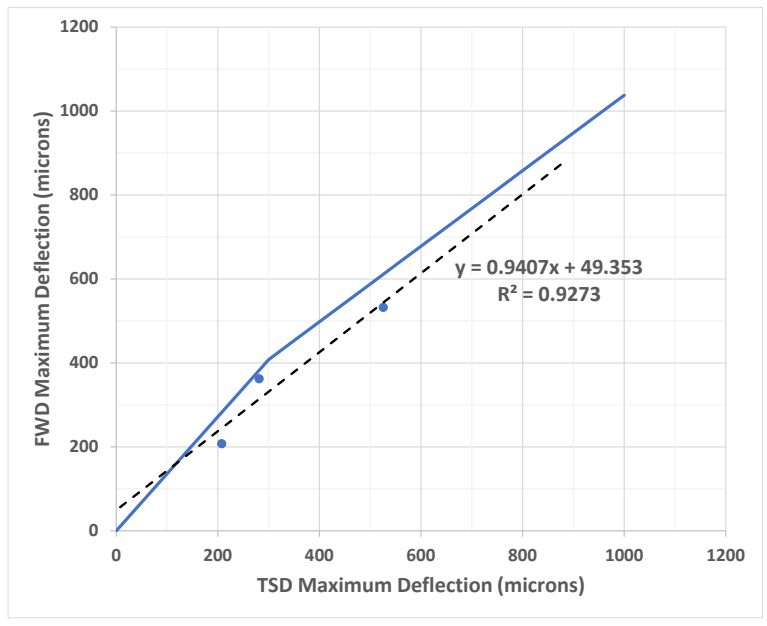


Figure 3.17: Comparison of TSD and FWD measurements after adjusted for radial distance: Run #9



By combining all the FWD and iPAVe data collected across all three instrumentation sites across Queensland and Western Australia, the general correlation relationship (maximum deflection and curvature) is shown in Figure 3.18 and Figure 3.19, respectively.

Figure 3.18: Correlation between the TSD and FWD maximum deflections at Deception Bay Road



-WD Curvature (microns) v = 1.002x $R^2 = 0.9866$ TSD Curvature (microns)

Figure 3.19: Correlation between the TSD and FWD curvature (D0-D200) at Deception Bay Road

# 3.7 Summary of Results

In this section, the raw data collected from the FWD, iPAVe and instrumentation array was analysed and compared. It was found that the embedded sensor array and the associated proposed analysis method can accurately track the pavement deflection (and velocity) when subjected both to impact loads (e.g. from an FWD) and a moving wheel load (e.g. from the rear axle of the iPAVe/TSD). The staggering array design allows the motion of the iPAVe to be tracked even if the vehicle's travel path deviates from the centreline of the array. There is reasonable agreement between the deflection measured by the instrumentation array and the measurement output from both the FWD and the iPAVe. The results also show some intrinsic variability between the multiple iPAVe runs in terms of the measured deflections, variability in applied dynamic loads, and its varying effect on the measured deflections when the iPAVe travels at different speeds.

To explain the magnitude differences between the different devices, the results in the radial distance domain were mapped (rather than the offset distance in the direction of travel). It was found that such an approach could partially explain the discrepancy measured by each device.

The data collected from the Deception Bay Road instrumentation site improved the correlation relationship established using the data collected from the earlier study in Western Australia. A revised correlation is proposed to correlate the maximum deflection (D<sub>0</sub>) and curvature (D<sub>0</sub>-D<sub>200</sub>) measured by an FWD and the iPAVe.

# 4 Live Traffic Measurement

The concept of using ground instrumentation to monitor the motion of iPAVe can easily be expanded for monitoring the live traffic travelling on Deception Bay Road. Figure 4.1 to Figure 4.4 show different types of vehicles captured during the project. The pavement response demonstrated that the current ground instrumentation array can reliably be used to capture the displacement of different classifications of vehicles. In the case of the iPAVe with a known weight, the displacement can easily be monitored over different periods. If other live traffic is monitored in combination with Weigh-In-Motion (WIM) technology, this can be expanded to monitor other vehicles types and its relative displacement (which is related to the pavement strains) of the selected pavement.

Figure 4.1: Typical passenger vehicle on Deception Bay Road



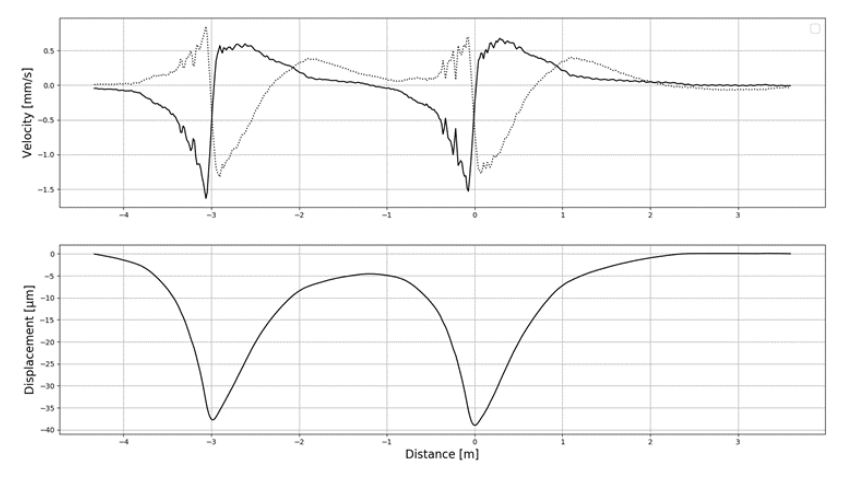
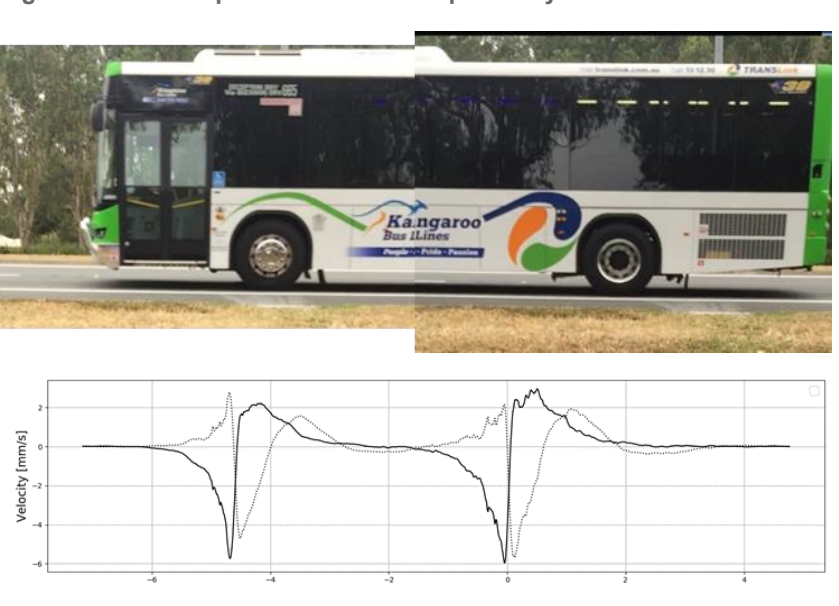


Figure 4.2: Example of an unladen three-axle group semi-trailer on Deception Bay Road



Figure 4.3: Example of a bus on Deception Bay Road



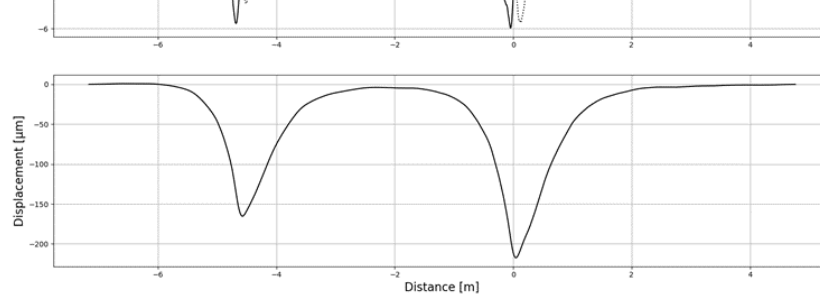
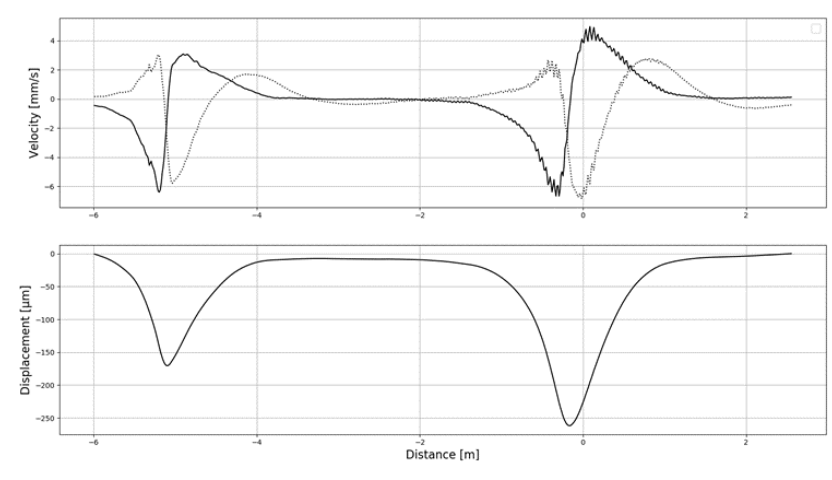


Figure 4.4: Example of a loaded flat-bed vehicle on Deception Bay Road





# 5 Use of TSD Data by Other Road Authorities

## 5.1 iPAVe User Group

In order to identify how different road agencies use TSD data, an iPAVe user group was formed to facilitate knowledge transfer across different iPAVe users. The first meeting was held on 20 November 2019.

Representatives from the following organisations participated:

- Transport and Main Roads Queensland (TMR)
- Main Roads Western Australia (MRWA)
- Roads and Maritime Services (RMS)
- Australian Road Research Board (ARRB).

Other road users include members from the Northern Territory, Victoria and South Australia. It is anticipated that future iPAVe user group meetings will include a representative from these organizations.

A summary of the topics presented is provided in Table 5.1.

Table 5.1: List of iPAVe user organisations that participated in the online forum held on 20 November 2019

Organisation	Topic
ARRB	Introduction – TSD users around Australia and New Zealand
ARRB & TMR	<ul> <li>TMR draft technical note TN 182</li> <li>Ground instrumentation work in Queensland (NACOE) and Western Australia (WARRIP)</li> </ul>
MRWA	MRWA current practice on the use of data visualisation and mobile app in assisting implementing TSD in maintenance planning
TfNSW	Use of TSD data in NSW
TMR	TMR practice on the use of TSD data

Based on the information obtained at the first User Group meeting, the current approaches to using TSD data by each organisation is summarised in the following sub-sections.

# 5.2 Transport and Main Roads Queensland (TMR)

Jeffrey Lee (ARRB) and Alan Conaghan (TMR) presented the latest developments in utilising the iPAVe at an online forum. First, a draft technical note titled *Deflection Testing of Roads with Traffic Speed Devices* (TN 182) was presented. The purpose of TN 182 is to provide information and guidance on the use of TSD technology in pavement condition assessment. The potential for the TSD to be used in pavement rehabilitation design is explored. The presentation was followed by an update of the ground instrumentation works conducted in Queensland and Western Australia.

# 5.3 Main Roads Western Australia (MRWA)

For asset management applications, a presentation titled *Use of TSD in MRWA Maintenance Decision Making* was presented at the User Group meeting. Based on the TSD measurement parameters, such as the maximum deflection  $D_0$  and Curvature ( $D_0$ - $D_{200}$ ), pavement risk index bins were proposed for each measurement parameter.

For example, the TSD deflection D<sub>0</sub> was used to:

- estimate the risk level of structural failure of an unbound granular pavement
- estimate the risk level of structural failure within a bound layer.

The TSD curvature function D<sub>0</sub>-D<sub>200</sub> was used to:

estimate the risk level of structural failure of the upper layer of a unbound granular pavement

estimate the fatigue life of an asphalt surface.

An example of the risk index proposed is shown in Table 5.2.

Table 5.2: Example of a proposed risk index based on the TSD measurement parameter presented by MRWA

TSD	100 00 000	Level of		of Risk	sk	
Parameter (micro)	Application	Low	Medium	High	Very High	
Deflection (D₀)	Estimate the risk level of structural failure of a <b>unbound</b> (incl. modified stabilised) granular pavement	≤500	>500 ≤800	>800 ≤1050	>1050	
Deflection (D <sub>0</sub> )	Estimate the risk level of structural failure of a pavement with <b>bound</b> layers (Hydrated cement treated crushed rock layer(s) or structural asphalt pavement layer(s))	≤300	>300 ≤500	>500 ≤650	>650	
Curvature (D <sub>0</sub> - D <sub>200</sub> )	Estimate the risk level of structural failure of the upper layer(s) of a unbound granular pavement	≤170	>170 ≤240	>240 ≤300	>300	
Curvature (D <sub>0</sub> - D <sub>200</sub> )	Estimate the fatigue life of an <b>asphalt</b> surface	≤130	>130 ≤180	>180 ≤220	>220	

Another development area includes a platform to visualise data on mobile devices, which will assist asset engineers and inspectors to highlight pavement areas with different level of risk and making the data available during site inspection.

# **5.4 Transport for New South Wales (TfNSW)**

During the User Group meeting, representatives from TfNSW gave a presentation titled *Use of Traffic Speed Deflectometer Data in NSW*. It is noted that iPAVe data is collected in NSW annually in most trafficked lanes and generally in the prescribed direction. At this stage, TSD data has not be used for pavement rehabilitation design.

# 6 Conclusions

The project scope for the current year study was to investigate the possible applications of iPAVe data. A technical note has been prepared to inform TMR Districts of possible applications of, and risks associated with the use of, iPAVE data. Currently, there are limited studies available in Australia which provide an understanding of the relationship between pavement response (i.e. deflection) and the performance of asphalt/granular pavements. The work conducted in Queensland supplemented a similar ground instrumentation site set up in Western Australia under the WARRIP research initiative.

This report has addressed the analysis of measurements conducted at a ground instrumentation site on Deception Bay Road near Brisbane under the NACOE project. The measurements have provided insight into the different pavement deflections measured by the FWD and the iPAVe. An attempt was made to present the deflection data in terms of the radial offset distance, and the use of this approach appeared to improve the discrepancy between the FWD and iPAVe measurements.

The main findings from the study are as follows:

- The embedded sensor array and the associated proposed analysis method can accurately track the pavement deflection (and velocity) when subjected both to impact loads (e.g. from an FWD) and a moving wheel load (e.g. from the rear axle of the iPAVe/TSD).
- The staggering array design allows the motion of the iPAVe to be tracked even if the vehicle's travel path deviates from the centreline of the array.
- There was reasonable agreement between the deflections measured by the instrumentation array and the FWD and iPAVe.
- There was some intrinsic variability between the multiple iPAVe runs in terms of the measured deflections, variability in applied dynamic loads, and its varying effect on the measured deflections when the iPAVe travelled at different speeds.
- In order to explain the differences in magnitude between the different devices, it was proposed that the results be mapped in the radial distance domain (rather than the offset distance in the direction of travel). It was found that such an approach could partially explain the discrepancies between each device.
- The analysis of the data collected at the Deception Bay Road instrumentation site resulted in an improvement in the correlation established using the data collected from the earlier study in Western Australia. A revised correlation between the maximum deflection (D<sub>0</sub>) and curvature (D<sub>0</sub>-D<sub>200</sub>) measured by an FWD and the iPAVe is proposed.

The study not only demonstrated that the instrumentation array can accurately measure the responses from FWD and iPAVe, it also demonstrated the practicality of the concept of using an instrumentation array to monitor a range of live traffic loadings, ranging from light vehicles to multiple-axle heavy vehicles.

Finally, the report presents details of the current utilisation of the iPAVe data by different Australian road agencies.

# References

- Austroads 2014, *Traffic speed deflectometer data review and lessons learnt*, prepared by J Roberts, U Ai, T Toole & T Martin, AP-T279-14, Austroads, Sydney, NSW.
- Lee, J & Duschlbauer, D 2019, 'Benefits of Traffic Speed Deflectometer data in pavement analysis (year 3)', contract report PRP 16119, prepared for Queensland Department of Transport and Main Roads under the NACoE program, ARRB, Port Melbourne, Vic.
- Lee, J, Duschlbauer, D & Chai, G 2019, 'Ground instrumentation for Traffic Speed Deflectometer (TSD)', contract report PRP17037-02, prepared by ARRB for WARRIP, WARRIP, Perth, WA.
- Muller, WB & Roberts, J 2013, 'Revised approach to assessing traffic speed deflectometer data and field validation of deflection bowl predictions', *International Journal of Pavement Engineering*, vol. 14, no. 4, pp. 388-402.
- Nasimifar, M, Thyagarajan, S, Siddharthan, RV & Sivaneswaran, N 2016, 'Robust deflection indices from traffic-speed deflectometer measurements to predict critical pavement responses for network-level pavement management system application', *Journal of Transportation Engineering*, vol. 142, no. 3, 11 pp.
- Pedersen, L 2013, 'Viscoelastic modelling of road deflections for use with the traffic speed deflectometer', PhD thesis, Technical University of Denmark, Lyngby, Denmark.
- Rasmussen, S, Aagaard, L, Baltzer, S & Krarup, J 2008, 'A comparison of two years of network level measurements with the Traffic Speed Deflectometer', *Transport research arena conference*, 2008, *Ljubljana, Slovenia*, European Commission, Brussels, Belgium, 8 pp.
- Zofka, A, Sudyka, J, Maliszewski, M, Harasim, P & Sybilski, D 2014, 'Alternative approach for interpreting traffic speed deflectometer results', *Transportation Research Record*, vol. 2457, pp. 12-8.

# **Bibliography**

- Austroads 2019, *Guide to pavement technology part 5: pavement evaluation and treatment design*, AGPT05-19, Austroads, Sydney, NSW.
- Nazarian, S & Bush, A 1989, 'Determination of deflection of pavement systems using velocity transducers', *Transportation Research Record*, vol. 1227, pp. 147-58.